

# Enhancing Field-Oriented Control of Electric Drives with Tiny Neural Network Optimized for Micro-controllers

Martin Joel Mouk Elele  
University of Pavia  
Pavia, Italy

Shixin Zhuang  
Mathworks  
Boston, USA

Danilo Pau  
STMicroelectronics Inc.  
Milan, Italy

Tullio Facchinetti  
University of Pavia  
Pavia, Italy

## ABSTRACT

The deployment of neural networks on resource-constrained micro-controllers has gained momentum, driving many advancements in Tiny Neural Networks. This paper introduces a tiny feed-forward neural network, TinyFC, integrated into the Field-Oriented Control (FOC) of Permanent Magnet Synchronous Motors (PMSMs). Proportional-Integral (PI) controllers are widely used in FOC for their simplicity, although their limitations in handling nonlinear dynamics hinder precision. To address this issue, a lightweight 1,400 parameters TinyFC was devised to enhance the FOC performance while fitting into the computational and memory constraints of a micro-controller. Advanced optimization techniques, including pruning, hyperparameter tuning, and quantization to 8-bit integers, were applied to reduce the model's footprint while preserving the network effectiveness. Simulation results show the proposed approach significantly reduced overshoot by up to 87.5%, with the pruned model achieving complete overshoot elimination, highlighting the potential of tiny neural networks in real-time motor control applications.

## KEYWORDS

Tiny Neural Networks, Micro-controllers, Permanent Magnet Synchronous Motor, Field-Oriented Control, Proportional-Integral Controller, Optimization

## 1 INTRODUCTION

Over the last decade, machine learning applications have expanded from traditional domains like computer vision to edge-centric problems such as near-sensor data analytics and intelligent control in resource-constrained environments. EdgeAI, previously known as TinyML, addresses this challenge by enabling machine learning inference on ultra-low-power devices, such as micro-controllers, which prioritize power efficiency, low latency, and minimal memory use [1]. This paradigm supports localized intelligent computation, reducing cloud dependency while enhancing privacy and efficiency [21]. Tiny Neural Networks (TinyNN) have shown potential in fields requiring rapid and efficient monitoring and control with low computational overhead [13]. Still, these cases have been focused on Internet of Things (IoT) and much less in domains such as electric vehicles (EVs), with particular reference to electric motor control.

Permanent Magnet Synchronous Motors (PMSMs), known for their high torque and power density, are pivotal in EV applications

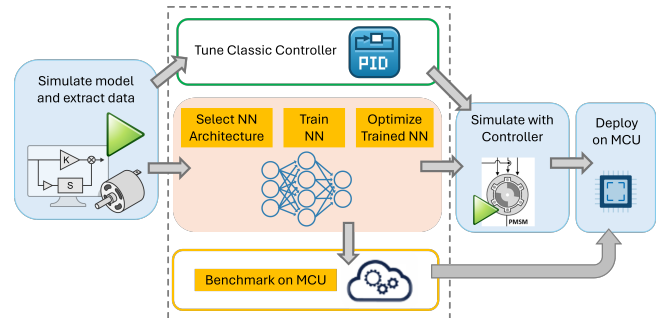


Figure 1: Workflow diagram to deploy NN-augmented FOC

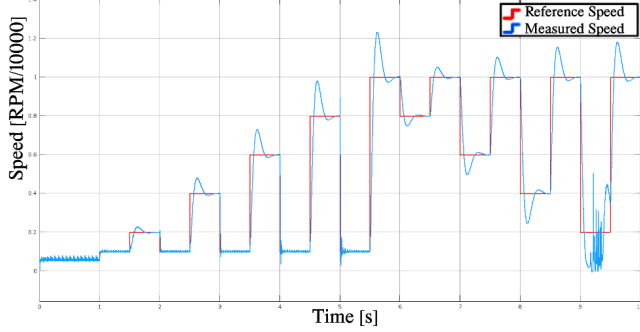
such as automotive, industrial, naval and aeronautics, where compact size and precision control are essential [19]. PMSMs consist of a stator housing the windings and a rotor containing permanent magnets. The operational interaction between the stator's rotating magnetic field and the rotor's fixed magnetic field enables synchronization at synchronous speed [10]. Field-Oriented Control (FOC) is a widely adopted technique to obtain good control capability over the full torque and speed range for various motor types, including PMSM.

Proportional-Integral (PI) controllers are simple and easy to implement but can be challenging to tune in situations where there are uncertainties and external disturbances. For example, in the case of PMSMs, electrical parameters such as resistance and inductance can change with wear and operating temperature, introducing uncertainties in system dynamics. To address the tuning challenges, advanced control techniques like  $H_\infty$ -synthesis [6] and Model Predictive Control (MPC) improve robustness but significantly increase control loop complexity [8], causing unacceptable latencies on resource-constrained Micro-Controller Units (MCUs).

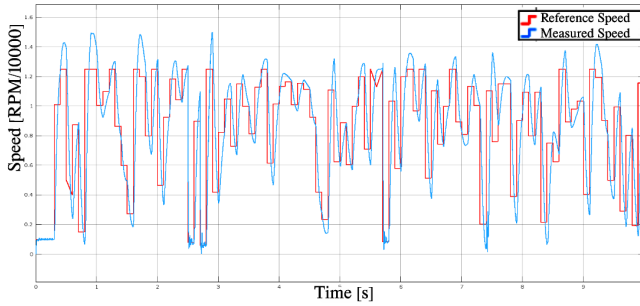
This work devises a tiny feed-forward Neural Network (NN), TinyFC, for FOC to enhance the responsiveness and precision of motor control systems. TinyFC, optimized for resource-constrained MCUs, provides improved performance while maintaining the strict power and memory constraints of embedded implementations. The design workflow of TinyFC is illustrated in Figure 1. Experimental results have been derived from two test cases specifically designed to test the controller in challenging operational scenarios. The results demonstrated that this approach can meet the demands of modern EV control applications, showcasing the NN-augmented controllers to efficiently address real-world challenges.



Test case 1 was designed to test the controller's response to a sequence of step signals with varying amplitudes [18], and introduces a signal with 2 transitions per second [16]. Tracking results using conventional PI-based FOC are shown in figure 3a.



(a) Case 1: Reference speed of step signals



(b) Case 2: Reference speed of step and ramp signals

Figure 3: Measured speed collected from PI-based FOC

In test case 2, the input signal is a combination of step and ramp signals [18] with 10 speed transitions per second, designed to assess the controller's ability to manage both abrupt changes and gradual variations in speed. For test case 2, the tracking accuracy of the PI controller is shown in figure 3b.

#### 4 TRAINING OF THE NEURAL NETWORK

Neural networks are trained to classify abstract patterns or predict outcome without having experience or existing knowledge to draw from. Our dataset simulates the behavior of a PMSM motor controlled using the FOC scheme, and it is made by the parameters reported in table 1.

Notation	Parameter	I/O
$\omega^{ref}$	Reference Speed	Input
$\omega^{meas}$	Measured Speed	Input
$i_q^{PI}$	PI-predicted Quadrature Current	Input
$\Delta i_q^{TinyFC}$	Current Compensation	Output

Table 1: Parameters composing the dataset used in the training of the NN model

PI-based FOC assumes precise predictions in the speed control loop in normal operation of PMSM. However, uncertainties and

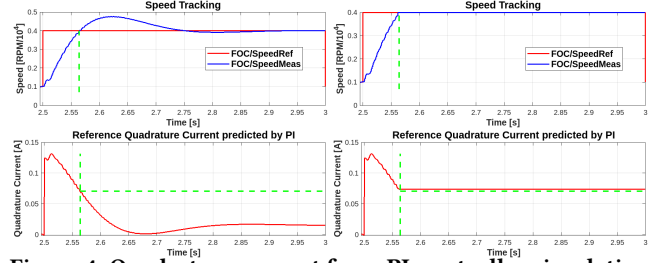


Figure 4: Quadrature current from PI-controller simulation adjusted using speed observations threshold

external disturbances, such as operating temperature or system dynamics, can lead to performance degradation for PI controllers [5]. In both cases described in section 3.2, the controller performed poorly. This happened when the calculated reference quadrature current generated by the speed PI controller contained deviations (errors) for most of the time steps. When the system dynamic changes, the PI controller demonstrates sluggish responses, overshoots, stability issues and tracking errors. To improve the quality of the ground truth signal, the prediction made by the PI controller in the speed control loop was adjusted to eliminate the sections containing overshoots. The remainder of this section discusses the impact of how the adjusting approaches affect the signals in the test cases.

In test case 1, simulations show that the PI controller struggle to quickly adapt to abrupt changes in the reference speed, leading to poor dynamic performances and sluggish responses. Moreover, it produces a significant deviation, as can be seen from the maximum deviation for PI-only control in table 3, and longer settling times, impacting the precision and stability of motor control. The PI controller exhibits oscillations before stabilizing, causing abnormal spikes in the predicted quadrature current. By analyzing the reference quadrature current and response speed, it was possible to identify when the quadrature current exceeded the desired range. This range was defined using a threshold  $C$ , representing the maximum acceptable value within the response interval [3]. The modified signal was thus determined by the following equation:

$$x^{adj}(t) = \min\{|x(t)|, C\} \quad (1)$$

where  $x^{adj}(t)$  is the saturated signal.

If the response signal  $x(t)$  exceeds the threshold  $C$  in magnitude, the signal saturates to  $C$  as shown in Figure 4.

In test case 2, simulations show that with an increased speed transition frequency, although the PI controller followed the overall speed trend, it significantly fails to stabilize around the desired speed (for each interval). The instability of the response signal, i.e., the measured speed, posed greater challenges, as shorter intervals of steady-state behavior reduced reliability. The proposed approach involves rectifying the reference quadrature current  $i_q^{PI}$ . By analyzing intervals where the measured speed matches the reference speed, the initial and final in-range values of the quadrature current are used to generate a rectified signal. This rectification employs an exponential decay, or growth curve, aligning the initial and final in-range values of the quadrature current with the start and end

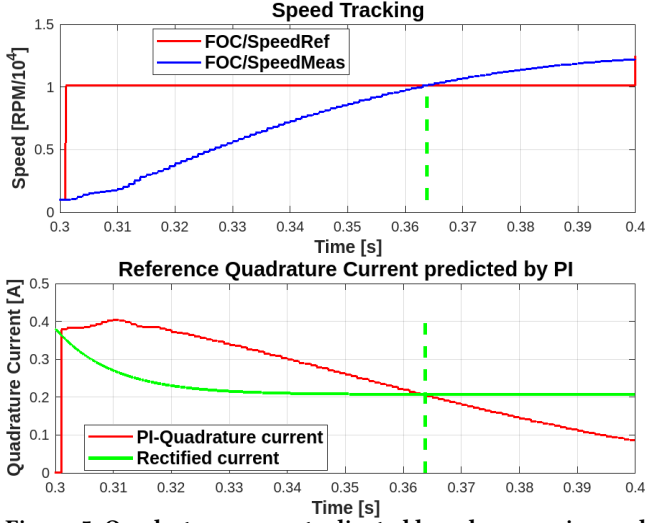


Figure 5: Quadrature current adjusted based on capping and rectification of measured speed

points of the function. The corrected signal ensures that the reference quadrature current more closely mimicks an ideal response, remaining within the desired range throughout each interval as shown in Figure 5. The corrected signal per interval hence becomes:

$$x^{adj}(t) = x^{final}(t) + (x^{initial}(t) - x^{final}(t))e^{-(t/\tau)} \quad (2)$$

where  $\tau$  is the decay constant ensuring that the current response is not too fast nor too slow, avoiding sharp oscillations in the response.

As a result of the previous considerations, the signal used as ground truth for training the TinyFC NN is  $\Delta i_q^{GT}$  defined as:

$$\Delta i_q^{GT} = x(t) - x^{adj}(t) \quad (3)$$

## 5 NEURAL NETWORK DESIGN

The TinyFC proposed in this work, whose architecture is shown in Figure 6, is a 1,400 parameter model prior deployed using the ST Edge AI Developer Cloud [25] to ensure deployability to the MCUs.

The model inputs/outputs are reported in table 1. The output of the TinyFC NN consists in the adjustment value  $\Delta i_q$  for the PI's prediction that is used to correct the reference signal  $i_q^{ref(PI)}$  based on the following equation:

$$i_q^{adj} = i_q^{ref(PI)} + \Delta i_q^{TinyFC} \quad (4)$$

where  $i_q^{adj}$  is the actual signal used for controlling the motor.

The model consists of branches of fully connected (FC) layers, combining 2 main-branches of 5 FC layers, and 2 residual FC layers per branch. The outputs of the two branches are merged using  $\tanh$  activations, constraining them to the range  $[-1, 1]$ . Training data comprised a  $300001 \times 4$  sequence per test case, derived from the Simulink PI-based FOC model. Each 10-second test case sampled at  $T_s = 3.3333 \times 10^{-5}$ , corresponding to the PWM switching frequency, yielding  $\sim 300,000$  samples. The NN was trained using data from the test case 1, and fine-tuned on data from test case 2. For training, the dataset was split into a training, validation and test set in the

ratio 8:1:1, in order to validate the model on unseen data. Once trained, the TinyFC was integrated into the FOC speed control unit, and its corrective performance was evaluated.

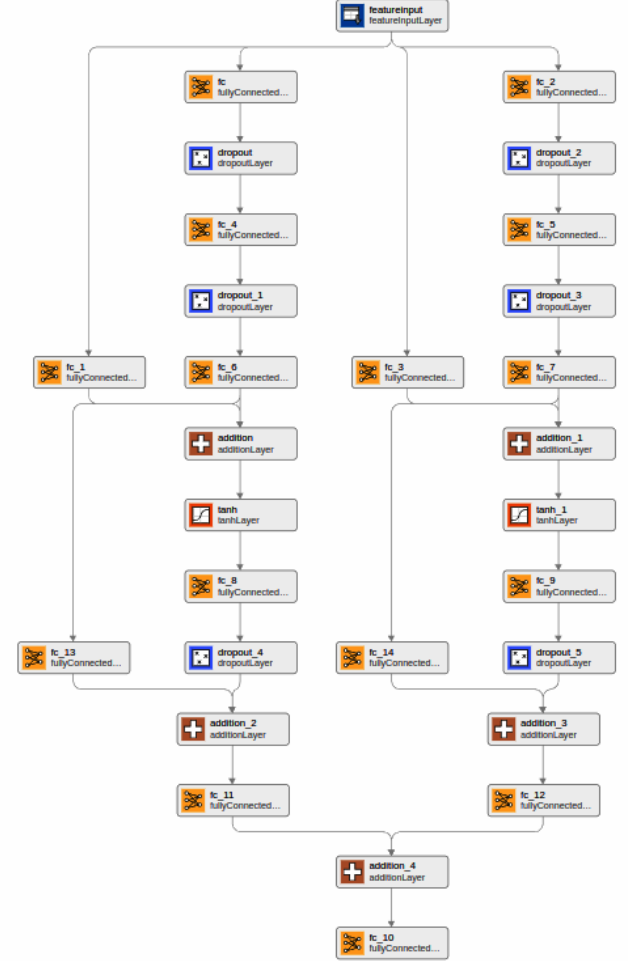


Figure 6: Network model topology as shown by MATLAB

A key challenge of integrating a NN in an FOC loop is its inference time, as the PWM operating at 30 kHz requires inputs every  $33.33 \mu\text{s}$ . If the NN's inference exceeds this time, system delays and performance issues may occur. To mitigate this, the NN was optimized by reducing the number of parameters, minimizing both computational and memory demands. Two alternative optimization approaches have been considered: hyperparameters optimization and pruning. In both cases, 8-bit quantization was applied to further reduce the memory footprint.

### 5.1 Hyperparameters optimization

Hyperparameters govern model performance. Therefore, hyperparameter optimization (HPO) is essential for optimal model performance and complexity. Using Bayesian Optimization (BO), which efficiently balances exploration and exploitation [15, 22], the model's hyperparameters were fine-tuned to achieve optimal predictions

Test Case	Model	Number of Parameters	MSE (%)
1	TinyFC	1,400	4.09
	HPO TinyFC	670	0.31
	Pruned TinyFC	873	9.19
2	TinyFC	1,400	0.62
	HPO TinyFC	340	0.62
	Pruned TinyFC	600	30.45

Table 2: Mean Squared Error of the trained NNs

for speed monitoring in PMSM FOC. This process identified the best-performing configuration for deployment.

## 5.2 Pruning

Projection pruning, leveraging Principal Component Analysis (PCA), was applied to compress the model by retaining only the most influential neurons based on variance in activations [28]. This reduced the model size by eliminating redundant connections while preserving accuracy. PCA-based pruning identified key neurons by solving an eigenvalue problem on the covariance matrix of standardized neuron activations [7].

## 5.3 Quantization

An additional step in the optimization process was quantization. All the models, i.e., the trained, HPO and pruned models, use a representation based on 32-bits floating point numbers. An integer 8-bit quantization was thus applied to further reduce the memory footprint of the model. Post training quantization (PTQ) was adopted by using ST Edge AI Developer Cloud [25].

## 6 EXPERIMENTAL RESULTS

To evaluate the performance of the devised TinyFC in the FOC loop, three sets of metrics are evaluated:

- Neural network metrics, i.e. accuracy
- Control loop metrics, i.e. deviation statistics
- Deployability metrics, i.e. inference time on MCU

### 6.1 Accuracy evaluation

To evaluate the predictive accuracy, comparing the NN's predictions to ground truth values derived from the modified quadrature current, the Mean Squared Error (MSE) is evaluated:

$$\text{MSE} = \frac{1}{n} \sum_{i=1}^n \left( \Delta i_q^{GT} - \Delta i_q^{\text{TinyFC}} \right)^2 \quad (5)$$

where  $\Delta i_q^{GT}$  is the ground truth (PI prediction error), and  $\Delta i_q^{\text{TinyFC}}$  is the NN's prediction. Model complexity, quantified by the number of learnable parameters, also plays a critical role, as it directly impacts computational efficiency and deployability.

Table 2 reports the evaluation of the MSE for the two considered test cases and the different configurations of optimized NNs.

The optimization procedure demonstrated a significant reduction in the model's parameters, achieving up to a 75.7% reduction in test case 2 with the HPO model. However, it is notable that while combining pruning with HPO could yield even fewer parameters, the HPO model did not perform satisfactorily within the FOC loop

Test Case	Controller	Max Deviation	Average Deviation	Max Overshoot
1	PI	0.81	0.05	0.24
	PI + TinyFC	0.89	0.02	0.03
	% Change	+9	-60	-87.5
2	PI	1.21	0.18	0.25
	PI + TinyFC	1.19	0.15	0.08
	% Change	-1.65	-16.7	-68

Table 3: Performance comparison between PI and the TinyFC NN in terms of max and average deviation and max overshoot

Test Case	Model	Max Deviation	Average Deviation	Max Overshoot
1	TinyFC	0.89	0.02	0.03
	HPO TinyFC	0.896	0.0316	0.06
	Pruned TinyFC	0.9	0.02	~ 0
2	TinyFC	1.19	0.15	0.08
	HPO TinyFC	1.23	0.15	1.24
	Pruned TinyFC	1.20	0.16	0.03

Table 4: Performance Comparison of Different Models

during this study (this case is not shown in this paper). Consequently, pruning was applied exclusively to the 1.4K-parameter TinyFC model for both test cases.

### 6.2 Control loop evaluation

The performance of the AI-augmented FOC was evaluated by monitoring overshoots and deviations during the simulations. The maximum overshoot represents the highest peak above the intended steady-state response, while deviation measures the difference between the reference and the controller's output. Maximum deviation identifies challenging control regions needing further optimization, while average deviation assesses overall tracking consistency [18].

The designed test cases expose the limitations with respect to FOC evaluation metrics. In test case 1, a noticeable overshoot occurs after each speed increase. In test case 2, the PI controller fails to stabilize. This latter effect is noticeable by comparing the performance of the PI controller in the two test cases, as can be seen in table 3: the signal diverges significantly from the reference speed, causing the maximum deviation to rise from 0.81 in the first case to 1.21, corresponding to a 49% increase. As observed in Figure 3b, there is a considerable delay between the reference signal's transition and the response of the measured speed, implying a lag in the system's ability to react instantaneously.

The TinyFC with 1,400 parameters was able to reduce the deviation in the control system between the reference speed signal and the measured speed signal, outperforming the PI-based FOC, with a maximum overshoot correction of up to 87.5% in test case 1, and 68% in test case 2, as shown in table 3. This comparison of the performance highlights the capacity on the NN to detect the error in the PI's prediction and correct it.

As explained in subsection 5.1, the TinyFC is optimized to obtain a lightweight model with a similar accuracy as the originally trained model. Table 4 shows that, inserting the HPO model in the control loop actually increases the overshoot by up to 100%, with the HPO model unable to properly grasp the relationship between its inputs and its expected output. The pruned model further enhances the

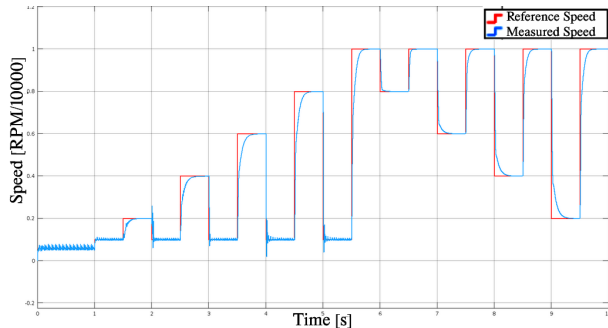


Figure 7: Output of pruned NN of test case 1

performance of the FOC, with  $\sim 100\%$  reduction in the overshoot (test case 1). The pruned model considerably reduces the overshoot in test case 2, despite slightly increasing the deviation from the reference signal in both cases. Despite the observed improvement in test case 2, the augmented FOC does not perform as well as in the test case 1, exposing some of the limitations of this approach.

### 6.3 Deployability on the MCU

Further validation is considered by deploying the models in the ST Edge AI Developer Cloud, an online farm where models can be tested on real MCUs.

The considered metrics for assessing the suitability of the proposed approach for the deployment on an MCU are:

- the number of multiplications and accumulations (MACC) required to run the model;
- the flash memory footprint to permanently store the application firmware;
- the RAM footprint, which is the dynamic memory needed to store intermediate results while running the model;
- the inference time required by the model to generate an output after an input is provided during real-time operations.

This work considered the deployability of the optimized TinyFC models on an off-the-shelf MCU, namely NUCLEO-G474RE, which is widely used for PMSM control in industrial and automotive applications, and FOC in particular. The primary objective was to ensure that the trained and optimized models meet the MCU embedded memory and real-time processing requirements for FOC.

The NUCLEO-G474RE development board, with STM32G4 MCU running at 170MHz, is specifically designed to strike a balance between processing power and energy efficiency, making it suitable for embedded control applications. With embedded 512 KiB of flash memory and 128 KiB of RAM [24], the NUCLEO-G474RE can handle moderately complex NN models.

Table 5 shows the comparative results of the different versions of the NN devised by this work, including the quantized version of the pruned model, which offered the best error correction in the FOC setup in Simulink. It is observable that, despite the pruned model having a lower MACC number and less parameters than the original model with 1,400 parameters, its inference time is surprisingly greater than that of the latter model, for both cases.

Test Case	Model	MACC	FLASH (KiB)	RAM (KiB)	Time ( $\mu$ s)
1	TinyFC	1620	Weights: 5.68 Lib: 15	Act: 0.199 Lib: 6	207.4
	HPO	764	Weights: 2.61 Lib: 15	Act: 0.152 Lib: 6	144.8
	Pruned	1034	Weights: 3.28 Library: 20	Act: 0.148 Lib: 10	232.2
	Quantized Pruned	910	Weights: 1.37 Lib: 32	Act: 0.383 Lib: 13	371.7
2	TinyFC	1620	Weights: 5.68 Lib: 15	Act: 0.199 Lib: 6	207.4
	HPO	470	Weights: 1.33 Lib: 15	Act: 0.105 Lib: 6	127.6
	Pruned	760	Weights: 2.26 Lib: 20	Act: 0.145 Lib: 10	215.2
	Quantized Pruned	640	Weights: 1.07 Lib: 32	Act: 0.360 Lib: 13	361.4

Table 5: Neural Network characteristics on NUCLEO-G474RE

### 6.4 Discussion

The challenge faced by the optimized models (HPO model in particular) implied that trimming less important weights or obtaining a model with the smallest MSE was not enough to guarantee the best performance in the FOC setup.

This was because MSE as the evaluation metric for the NN during training and validation was not enough to capture how a specific change in quadrature current can affect the stability of the system. Hence, a more robust indicator was required, which would take into account the physics (physical loss) related to the system for each prediction of the NN. Overall, the results from the TinyFC and its pruned version clearly showcase the benefits of using a NN in the control loop, which considerably reduces the deviations and overshoot that are generated due to the limitations of the PI controller.

The PI-based FOC, without the TinyFC, shown signs of underdamping, due to the presence of the overshoots and oscillations. The non-optimized TinyFC does reduce the oscillations, which could be interpreted as adjustments in damping [4], since the oscillations in the speed response were reduced. The pruned model further reduced them.

## 7 CONCLUSIONS

This research demonstrated the potential of TinyNN to improve FOC by minimizing overshoots and tracking errors in PI-based control. By leveraging reference speed, measured speed, and the PI controller's output, the proposed TinyFC model enhanced speed tracking and reduced steady-state errors. However, optimizing TinyFC inference for MCU timing remains a challenge. Limitations in using MSE suggest exploring physics-informed neural networks (PINNs) to better model input dependencies through physics-based loss functions [2, 27]. While effective, the approach depends on the PI controller for reference adjustments, limiting TinyFC to a supportive role.

Future works could focus on developing a fully data-driven TinyNN model to replace the PI controllers, achieving a unified control system free from traditional methods.

## REFERENCES

- [1] Youssef Abadade, Anas Temouden, Hatim Bamoumen, Nabil Benamar, Youssa Chtouki, and Abdelhakim Senhaji Hafid. A comprehensive survey on tinyml. *IEEE Access*, 11:96892–96922, 2023.
- [2] Shaikhah Alkhadhr, Xilun Liu, and Mohamed Almekkawy. Modeling of the forward wave propagation using physics-informed neural networks. In *2021 IEEE International Ultrasonics Symposium (IUS)*, pages 1–4, 2021.
- [3] J. Allison. The linear rectification of two amplitude-modulated signals and noise. *IEEE Transactions on Information Theory*, 13(1):69–75, 1967.
- [4] A.G. Atkins and M. Escudier. *A Dictionary of Mechanical Engineering*. Oxford Paperback Reference. OUP Oxford, 2013.
- [5] Grzegorz Bialic and Marian B?achuta. *Developments in the Control Loops Benchmarking*, 05 2008.
- [6] Runze Cai, Ruixiang Zheng, Ming Liu, and Mian Li. Optimal selection of pi parameters of foc for pmsm using structured h-infinity-synthesis. In *IECON 2017 - 43rd Annual Conference of the IEEE Industrial Electronics Society*, pages 8602–8607, 2017.
- [7] Y. Chen, S. Hu, and D. Chen. Fast pruning strategy for neural network size optimization and its applications. *Journal of Chemical Industry and Engineering (China)*, pages 522–526, 2001.
- [8] Cahyantari Ekaputri and Arief Syaichu-Rohman. Model predictive control (mpc) design and implementation using algorithm-3 on board spartan 6 fpga sp605 evaluation kit. In *2013 3rd International Conference on Instrumentation Control and Automation (ICA)*, pages 115–120, 2013.
- [9] Kurt Hornik, Maxwell Stinchcombe, and Halbert White. Multilayer feedforward networks are universal approximators. *Neural Networks*, 2(5):359–366, 1989.
- [10] Natthawut Kongchoo, Phonsit Santiprapan, and Nattha Jindapetch. A mathematical model and pi controller design based on indirect vector control for permanent magnet synchronous motor. *ECTI Transactions on Computer and Information Technology (ECTI-CIT)*, 16:260–267, 06 2022.
- [11] Paul C. Krause, Oleg Wasynczuk, and Scott D. Sudhoff. *Reference-Frame Theory*, chapter 3, pages 86–120. John Wiley & Sons, Ltd, 2013.
- [12] Suryakant A. Kuvalekar and S.R. Mohanrajan. Pmsm torque ripple reduction in electric vehicle using neural network. In *2021 IEEE International Power and Renewable Energy Conference (IPRECON)*, pages 1–6, 2021.
- [13] Ji Lin, Ligeng Zhu, Wei-Ming Chen, Wei-Chen Wang, and Song Han. Tiny machine learning: Progress and futures [feature]. *IEEE Circuits and Systems Magazine*, 23(3):8–34, 2023.
- [14] Minh Tri Lê, Pierre Wolinski, and Julyan Arbel. Efficient neural networks for tiny machine learning: A comprehensive review, 2023.
- [15] MathWorks. Bayesian optimization. <https://uk.mathworks.com/help/stats/bayesopt.html>, 2024.
- [16] Juan Camilo Nustes, Danilo Pietro Pau, and Giambattista Gruosso. Field oriented control dataset of a 3-phase permanent magnet synchronous motor. *Data in Brief*, 47:109002, 2023.
- [17] Juan Camilo Nustes, Danilo Pietro Pau, and Giambattista Gruosso. Modelling the field oriented control applied to a 3-phase permanent magnet synchronous motor. *Software Impacts*, 15:100479, 2023.
- [18] Katsuhiko Ogata. *Discrete-Time Control Systems*. Prentice Hall, Australia, Sydney, 1987.
- [19] Preeti Osekar, Sahana Kalligudd, Sachin Angadi, and A B Raju. Field oriented control of surface-mount pmsm using model predictive current control. In *2022 IEEE North Karnataka Subsection Flagship International Conference (NKCon)*, pages 1–5, 2022.
- [20] M. Abdes S. K. Khan and M. Azizur Rahman. An adaptive self-tuned wavelet controller for ipm motor drives. In *2008 IEEE Power and Energy Society General Meeting - Conversion and Delivery of Electrical Energy in the 21st Century*, pages 1–4, 2008.
- [21] Muhammad Shafique, Theocharis Theocharides, Vijay Janapa Reddy, and Boris Murmann. Tinyml: Current progress, research challenges, and future roadmap. In *2021 58th ACM/IEEE Design Automation Conference (DAC)*, pages 1303–1306, 2021.
- [22] Somnath Sinha, Shirasthi Choudhary, and Aditi Paul. A novel two-step bayesian hyperparameter optimization strategy for dos attack detection in iot. In *2024 2nd International Conference on Intelligent Data Communication Technologies and Internet of Things (IDCIoT)*, pages 112–119, 2024.
- [23] STMicroelectronics. Motor control nucleo pack with nucleo-f302r8 and x-nucleo-ihm07m1. <https://www.st.com/en/evaluation-tools/p-nucleo-ihm001.html>. Last accessed: November 10, 2024.
- [24] STMicroelectronics. Stm32 nucleo-64 development board with stm32g474re mcu. <https://www.st.com/en/evaluation-tools/nucleo-g474re.html>. Last accessed: November 10, 2024.
- [25] STMicroelectronics. St edge ai developer cloud. <https://stedgeai-dc.st.com/home>, 2024.
- [26] Jonathan Tacke, John F. O'Brien, and Dakota Roberson. Auto-synthesis of high-performance power system compensators. *IEEE Transactions on Power Systems*, 38(2):1219–1228, 2023.
- [27] Nathaniel Trask, Andy Huang, and Xiaozhe Hu. Enforcing exact physics in scientific machine learning: A data-driven exterior calculus on graphs. *Journal of Computational Physics*, 456:110969, 2022.
- [28] Lei Xie, Quan-Ling Zhang, Ming Guo, and Shu-Qing Wang. Linear pruning techniques for neural networks-based on projection latent structure. In *SMC'03 Conference Proceedings. 2003 IEEE International Conference on Systems, Man and Cybernetics. Conference Theme - System Security and Assurance (Cat. No.03CH37483)*, volume 2, pages 1304–1309 vol.2, 2003.